Hindawi
Shock and Vibration
Volume 2021, Article ID 5850073, 13 pages
https://doi.org/10.1155/2021/5850073

Research Article

Seismic Performance of CFST Frame-Steel Plate Shear Walls Connected to Beams Only

Qin Rong,[1] Zhonghui Zhao,[1] Lanhui Guo,[2] Xiaomeng Hou ,[2] Li Lin ,[1] and Hongtao Bi[1]

[1]*School of Architecture and Civil Engineering, Harbin University of Science and Technology, Harbin 150080, China*
[2]*Key Lab of Structures Dynamic Behavior and Control of the Ministry of Education, Harbin Institute of Technology, Harbin 150090, China*

Correspondence should be addressed to Xiaomeng Hou; houxiaomeng@gmail.com and Li Lin; 13766899951@163.com

Received 12 May 2021; Accepted 4 August 2021; Published 14 August 2021

Academic Editor: Trupti Ranjan Lenka

The safety and cost of structures composed of concrete-filled steel tube (CFST) frame-steel plate shear walls (SPSWs) with two-side connections are governed by the seismic performance. The response modification factor R and displacement amplification factor C_d are important seismic performance factors. In this paper, nonlinear seismic responses of 10-story, 15-story, and 20-story CFST frame-SPSWs (CFST-SPSWs) are studied. A nonlinear finite element model which includes both material and geometric nonlinearities is developed using the finite element software OpenSees for this study. The accuracy of model was validated by comparing with experimental results. Nonlinear seismic analysis shows that CFST-SPSWs, in high seismic region, behave in a stable and ductile manner. Also, R and C_d of CFST-SPSWs were evaluated for the structure models using incremental dynamic analysis (IDA), and the average values of 3.17 and 3.05 are recommended, respectively. The recommended R value is greater than the value (2.8) in the "Chinese Code for seismic design of buildings" for composite structures, indicating the code is conservative. The structural periods provided by current code are generally lower than the periods calculated by finite element analysis. Research results show that R and C_d increase with increasing story number, span number, and structural period. Ductility reduction factor R_μ increases with increasing span number and decreasing story number. Overstrength factor R_s increases with increasing story number and decreasing span number.

1. Introduction

Increasing material strength and deformation properties and using composite structures are two effective methods of improving the seismic performance of building structures [1]. Steel plate shear walls with composite columns and infill plates connected only to beams are important types of composite structures with high seismic performance. Current seismic design methods are primarily based on load-carrying capacity. Currently, in order to ensure structures into inelastic phase, seismic action (horizontal base shear) in design is determined by reducing the elastic seismic force using the response modification factor R for structural seismic acceleration ("moderate earthquake" in Chinese seismic fortification intensity). The R is governed by structural overstrength performance, ductility, and energy dissipation. The structural inelastic degree depends directly on a reduced seismic force, and reduction factor values are concerned with seismic action in design. In the performance-based seismic design method, the inelastic response spectrum is widely applied in the displacement-based design method. In this method, the inelastic response spectrum is obtained by using response modification factor to reduce the elastic response spectrum. Therefore, the structural response modification factor is one of the most crucial parameters in structural seismic design.

The structural response modification factor values from various seismic codes around the world are different. In Chinese code, the "General rule for performance-based seismic design of buildings" (CES160 : 2004) [2] (following shorted form is "General rule") lists some of the structural response modification factors within a structural system;

however, the "Code for seismic design of buildings" (GB50011-2010) [3] uses information frequently collected during earthquakes to calculate seismic action. The connotative structural response modification factor is 2.8, which neglects the difference between seismic performance and plastic deformation capacity within the system. Structural response modification factor values in American code were studied and compared with Japanese code by Uang [4] and Whittaker et al. [5]. The reinforced concrete structure designed according to EC8 (Eurocode 8: Design of structures for earthquake resistance) was evaluated in terms of behavior coefficient by Elnashai and Broderick [6], who found that the structural behavior coefficient of European code is conservative. The behavior factor of steel frame structure was analyzed by Kim and Choi [7]. The response modification factors of 20 buckling restrained braced frames (BRBFs) and 30 concentric braced frames (CBFs) were evaluated using Pushover analysis [8]. The response modification factors for CBFs were lower than the BRBF values. The response modification factors for CBFs ranged from 4.10 to 6.10 and ranged from 7 to 22 for BRBFs. The response modification factors of BRBFs with type *V*, inverted *V*, diagonal, and split *X* restrained bracing configurations were calculated using OpenSees software [9]. The response modification factors for BRBFs ranged from 7 to 9.4. The response modification factors of steel moment-resisting frames were calculated using different pushover analysis methods [10]. The response modification factors for steel moment-resisting frames ranged from 3.3 to 3.8, and the maximum difference for response modification factors calculated by adaptive pushover analysis (APA) method and conventional pushover analysis (CPA) method was 16%. The response modification factors of X-braced steel frames with different boundary conditions were calculated using pushover analysis methods using Sap2000 software [11]. The response modification factors for X-braced steel frames ranged from 4.3 to 11. The response modification factors varied with different boundary conditions. The response modification and overstrength factors in moment-resisting steel frames (MRSFs) with added triangular-plate damping and stiffness devices (TADAS) were evaluated using OpenSees software [12]. The response modification factors for MRSFs with TADAS were 15.9, and the factors for MRSFs with TADAS were greater than the MRSFs values. The response modification of steel slit panel-frames was evaluated using pushover analysis and nonlinear incremental dynamic analysis (NIDA) [13]. The response modification factors for steel slit panel-frames ranged from 6.14 to 8.11. The response modification factors calculated using pushover analysis are smaller than those derived from NIDA.

Apart from the steel structures [14, 15], the response modification factors of reinforced concrete structures were also investigated [16–19]. The response modification of reinforced concrete frames was evaluated using incremental dynamic analysis (IDA) [20]. The response modification factors $R = 6$ satisfied the expected safety level-against earthquake-induced collapse. The $R = 3$ value in current Chinese codes [2] is conservative for RC frames. The seismic behavior and failure mechanism of elevated concrete tanks with shaft and frame staging were evaluated using finite element (FE) modeling [21]. The response modification factors for elevated concrete tanks were 1.5–3, less than the recommended value of 3 by ACI 371R-08 [22]. The values of structural response modification factors for a reinforced concrete frame structure were evaluated based on Indian code by Mondal et al. [23]. The value in Indian code was greater than the actual value, meaning that the code was not safe.

Cyclic loading tests on four steel frames assembled with concrete-filled steel tubular (CFST)-bordered composite walls were conducted by Cao et al. [24]. Test results showed that the seismic performance of steel frame was improved by CFST-bordered composite wall. As compared with steel frame, the displacement ductility factor of steel frame CFST-bordered composite wall was reduced from 2.6–3.4 to 1.3–1.8. This is mainly because with the increase in steel ratio, the increase in the damage displacement is lower than that of yield displacement. Five steel-concrete-steel composite shear walls with J hook connectors (SCSSWJ) and boundary CFST columns under cyclic loading were conducted by Yan et al. [25]. Test results showed that the failure mode of SCSSWJs was flexure, which indicated the SCSSWJs exhibit good seismic performance.

Recently, our research group conducted seismic behavior tests on steel plate shear walls (SPSWs) and concrete filled steel tube (CFST) columns [26, 27]. The SPSWs exhibited acceptable hysteretic responses under cyclic loading. Literature review shows that the structural response modification factors of reinforced concrete and steel frame structure were studied. However, the research regarding the CFST frame-SPSW response modification factor was limited [28, 29]. To answer this question, the seismic performance of CFST frame-SPSWs is evaluated using the IDA method in this paper. Evaluating structural response modification factor systematically in a composite structural system of CFST frame-SPSWs will improve the seismic design and economy of engineering structures. The influence of story number, span number, and structural period on structural response modification factor R, ductility reduction factor R_μ, overstrength factor R_s, and displacement amplification factor C_d is analyzed. The reasonable values are presented for the CFST frame-SPSWs to provide a base value for the corresponding code.

2. CFST Frame-SPSWs Modeling

In order to evaluate the response modification factor R, ductility reduction factor R_μ, overstrength factor R_s, and displacement amplification factor C_d, CFST frame-SPSWs models were built using OpenSees.

2.1. Definition of Structural Response Modification Factor R. R is the ratio of the minimum strength to designed strength required to keep a structure fully elastic during a moderate earthquake. This coefficient is concerned with ductility and energy dissipation capacity, and it is an important coefficient for structural seismic design. C_d is the ratio between the

maximum elastic-plastic deformation and displacement calculated by elastic analysis according to the reduced seismic effect at the same intensity level during a moderate earthquake. Using the displacement amplification factor, the largest inelastic displacement of the structure can be estimated by determining the elastic displacement generated by seismic action.

The elastic-plastic deformation of a structure during an earthquake is shown in Figure 1. The nonlinear curve is simplified using a bilinear elastic-plastic curve. The structural response modification factor R and displacement amplification factor C_d are calculated as follows:

$$\begin{aligned} R &= \frac{V_e}{V_d} \\ &= \frac{V_e}{V_y}\frac{V_y}{V_d} \\ &= R_\mu R_s, \\ C_d &= \frac{\Delta_{\max}}{\Delta_d}. \end{aligned} \tag{1}$$

In formula (1), V_e is the maximum base shear when the structure remains completely elastic under moderate earthquake; V_y is the base shear when the structure yields; V_d is the designed base shear; Δ_d is the top horizontal displacement related to the designed base shear; Δ_y is the top horizontal displacement when the structure yields; $\Delta_{\max}$ is the maximum top horizontal displacement of the structure during a moderate earthquake; R_μ is the structural ductility reduction factor; and R_s is structural overstrength factor.

2.2. Structural Response Modification Factor Modeling Process. The process for calculating the structural response modification factor R and displacement amplification factor C_d of the CFST frame-SPSWs using IDA is as follows:

(1) The structural analysis model was designed, and the corresponding design-based shear V_d is solved according to the current domestic design code. The base shear method was used to analyze structures less than 40 m in height, and the mode decomposition method is used to analyze structures greater than 40 m in height.

(2) The CFST frame-SPSWs analysis model was built by using the finite software OpenSees based on the equivalent bars model of steel plate shear walls. Using the IDA method, the seismic response of real structures under the action of one artificial wave and multiple natural ground shocks was analyzed. The maximum base shear, top displacement, and interstory drift of the structure under different seismic levels were obtained by constantly adjusting the acceleration amplitude to analyze IDA. The curve of maximum base shear and top displacement under varying seismic was drawn and analyzed.

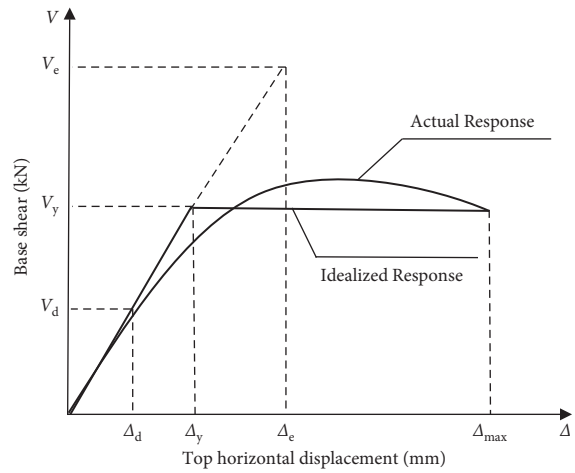

Figure 1: General structural response.

(3) Adjusting seismic peak acceleration of earthquake waves to the peak seismic acceleration under fortification seismic and conducting the time-history analysis of elastic structures, the maximum base shear V_e of elastic structures under fortification seismic was calculated. Then, structural response modification factor R was calculated according to the ratio of maximum base shear V_e to designed base shear V_d.

(4) Adjusting seismic peak acceleration to seismic fortification peak acceleration can get the maximum top displacement of the structure. According to the ratio of $\Delta_{\max}$ to the design top displacement Δ_d of the elastic structure, the displacement amplification factor C_d could be calculated during various amounts of ground shaking. The average value of C_d is used as the analysis result.

3. Modeling and Validation of CFST Frame-SPSWs Using the Equivalent Bars Model

To simplify the CFST frame-SPSWs model, the steel plate shear walls can be considered as the equivalent bars model. Steel plate shear walls and equivalent bars provide the same shear force capacity and same horizontal stiffness. The SPSWs with two-side connections are regarded as bidirectional crossbar. The specifics of the methods can be found in [28]. The analytical model of the CFST frame-SPSWs composite structure with two-side connections was developed using the finite element software OpenSees. The core concrete [29, 30] was simulated using the Concrete02 model based on Kent–Scott–Park provided in OpenSees. The stress-strain relationship was confirmed using a concrete constitutive model under axial compression and bending. Steel tubes and beams were modeled using the Steel02 model based on Giuffre–Menegotto–Pinto in OpenSees [31]. The Bauschinger effect can also be considered using the Steel02 model. The softening rate from elastic to plastic phase in this model is $R_0 = 18$, $a_1 = 0.925$, and $a_2 = 0.15$, respectively. Compressive and tensional yield stresses were considered

equal to steel yield stress. The nonlinear beam-column element and fiber sections were used to simulate the CFST columns and steel beams. This element considers some characteristics like plastic, stress strengthening, large strain, and large deformation. Steel02 material with 2% strain-hardening is used for these fibers.

The nonlinear beam-column element was used to simulate the CFST columns and steel beams. This element considers some characteristics like plastic, stress strengthening, large strain, and large deformation. The simplified bar model was adopted to simulate SPSWs with two-side connections, which allowed for the use of a shell element. The disadvantages of large amount of calculation and difficult in convergence can be avoided. This model uses two crossed steel bars to simulate the performance of SPSWs with two-side connections, and the two crossed steel bars have the same SPSWs hysteretic model under the tensile and compressive load. The two crossed steel bars were simulated using the Truss element in OpenSees, and the *hysteretic uniaxial* material is used to define the tension and compressive properties of simplified bars. The crossed steel bars hysteric model was determined using SPSWs hysteretic curves with characteristic points on corresponding skeleton curves and damage factors. The damage parameters "*damage*1" and "*damage*2" represent the damage of the material in every consecutive cycle in terms of ductility and energy, respectively. These parameters are considered as 0.005 and 0.01. The hysteretic uniaxial material also requires inputting the pinching parameters '*pinchx*' and '*pinchy*,' which was defined as follows [29]:

$$\begin{aligned} \text{pinchy} &= 0.07\ \ln\left(\frac{L}{H}\right) - 0.11\ \ln(\lambda) + 0.8, \\ \text{pinchx} &= 1.20\left(\frac{\lambda}{100}\right)^{0.44} - 0.17\left(\frac{\lambda}{100}\right) - 0.98, \end{aligned} \tag{2}$$

where L is the length of SPSW, H is the height of SPSW, and λ is the height-to-thickness ratio of SPSW.

The hysteretic performance tests of CFST frame-SPSW (specimens F2SW) and CFST frame (specimen CFST) conducted in Ref [26] were selected to validate the numerical model. The dimensions of specimens are shown in Table 1. The thickness and width, t and L_1, of SPSW are 3 mm and 1100 mm, respectively. The measured yield strength and tensile strength of steel are 290 MPa and 421 MPa, respectively. By conducting the same loading as experiment as in the model, the calculated shear force at the F2SW and CFST base columns can be obtained. The comparison of hysteretic curves for F2SW and CFST obtained from the experiment by Guo et al. [26] and the simulations from this study are shown in Figure 2. The stiffness of loading and unloading in the hysteretic curve seems credible as the calculated curves and test curves are consistent. The measured peak load is slightly greater than the calculated peak load. In order to enhance the connection of steel beams and shear walls, each steel plate was attached to beams of the boundary frame through 6 mm thick fishplates. Length of each fishplate was the same as that of the infill plate. In the finite element model, the contribution of the fishtail plate is difficult to simulate. Hence, the load-carrying capacity in the experiment is slightly greater. To summarize, the finite element model can analyze the hysteretic performance under cyclic load of the CFST frame-SPSWs.

4. Evaluating Structural Seismic Performance Using the IDA Method

In this study, the numerical model developed in Section 2 was used to evaluate the structural seismic performance of CFST frame-SPSWs. Six planar structural models were designed with 10, 15, and 20 stories, respectively, and the influence of story number, span number, and structural period on the structural response modification factor R is studied. These buildings are located in 9 seismic precautionary intensity zone, and designed basis seismic acceleration is 0.4 g. In addition, using Chinese code [2], these buildings' site classifications were selected as class 2, and their earthquake classification was selected as group one. Each model's height and span are 3.6 m and 6m, with the span numbers of 3 and 5, respectively. In addition, SPSWs were designed with the span-to-depth ratio of 1.0 and were settled at the midspan of the frame. The steel of the SPSW is Q235, and the steel of the frame beams and CFSTs is Q345. Q235 and Q345 mean that the standard yield strength of steel is 235 MPa and 345 MPa, respectively, as per the Standard for design of steel structures (GB 50017-2017). The core concrete grade in the steel-tube columns is C50 (compressive strength design value of 23.1 MPa). The floors are east-in-place reinforced concrete with a thickness of 100 mm and concrete grade of C30 (compressive strength design value of 14.3 MPa). C50 and C30 mean that the standard cube compressive strength of concrete is 30 MPa and 50 MPa, respectively, as per the Code for design of concrete structures (GB50010-2010).

The dead load of floor and roof is 4.2 kN/m2 and 4.6 kN/m2, respectively. The live load is 2 kN/m^2. The dead load and live load are calculated according to load code for the design of building structures (GB50009-2012). The frames were designed according to the "Code for seismic design of buildings," and the cross section dimensions are listed in Table 2.

By comparing the acceleration response spectrum in seismic records with Chinese code, 8 seismic records including 7 ground motion records and 1 artificial seismic wave were selected from the 22 available long field ground motion records, which are recommended in FEMA P695. According to the spectrum characteristics, amplitude, and duration of seismic records, the selected seismic records are similar to the site design spectrum, and the 8 seismic records are selected. The 8 seismic records (as listed in Table 3) were used in CFST frame-SPSWs seismic response evaluation using the IDA method. The peak accelerations of seismic records are amplified or reduced in proportion to ensure that the adjusted peak accelerations of seismic records satisfy the requirements of the highest value of acceleration time-history curves under the corresponding seismic levels in Chine code. Using this method, only the highest value in the seismic response spectrum is changed but the spectral characteristics remain the same.

Table 1: Dimension of specimens.

H (mm)	L (mm) L_1 (mm) t (mm)	$D \times t$ (mm)	Middle beam (mm)	Top and bottom beam (mm)
1500	2000 1100 3	219 × 4	H194 × 150 × 6 × 9	H300 × 150 × 6 × 9

Note. The Chinese designation of H shapes corresponds to the United States designation of W shapes and reflects member depth, width, web thickness, and flange thickness (unit in mm), respectively. The columns were CFSTs, the steel tube with a diameter of D and depth of t (unit in mm).

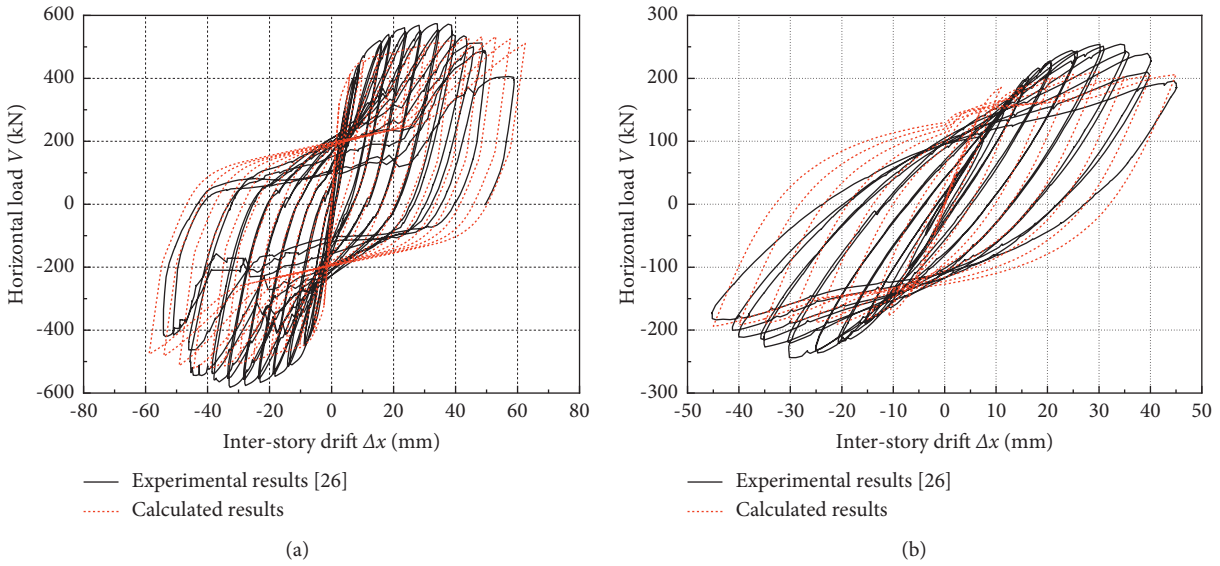

Figure 2: Comparison of experimental and calculated results: (a) specimen F2SW; (b) specimen CFST.

Table 2: Model dimensions.

Model number	Floor number	Column $D \times t$ (mm)	Beam (mm)	Steel plate depth (mm)
M-10-3	1–3	450 × 10	H500 × 300 × 11 × 15	8
M-10-5	4–6	400 × 9	H600 × 300 × 12 × 20 (HBE)	6
	7–10	350 × 8		6
M-15-3	1–5	500 × 12	H500 × 300 × 11 × 15	10
M-15-5	5–10	450 × 10	H600 × 300 × 12 × 20 (HBE)	8
	11–15	400 × 9		6
M-20-3	1–5	600 × 16	H500 × 300 × 11 × 15	12
	6–10	550 × 15		10
M-20-5	11–15	500 × 12	H600 × 300 × 12 × 20 (HBE)	8
	16–20	450 × 10		6

Note. Six planar structural models were designed with 10, 15, and 20 stories. The M-10-3 means the model has 10 stories and 3 spans. The HBE is horizontal boundary elements connected to shear walls. The beams were H-shaped steels and reflect member depth, width, web thickness, and flange thickness (unit in mm), respectively. The columns were CFSTs, and the steel tubes reflect diameter of D and depth of t (unit in mm).

Table 3: Information from the selected earthquake records.

Number	Level	Year	Name	Recording station
GM1	6.5	1979	Imperial Valley	Delta
GM2	6.5	1979	Imperial Valley	EI Centro Array #11
GM3	6.9	1989	Loma Prieta	Capitola
GM4	6.9	1989	Loma Prieta	Gilroy Array #3
GM5	7.4	1990	Manjil, Iran	Abbar
GM6	7.0	1992	Cape Mendocino	Rio Dell Overpass
GM7	6.6	1971	San Fernando	LA-Hollywood Stor Lot,090
GM8			Artificial waves	

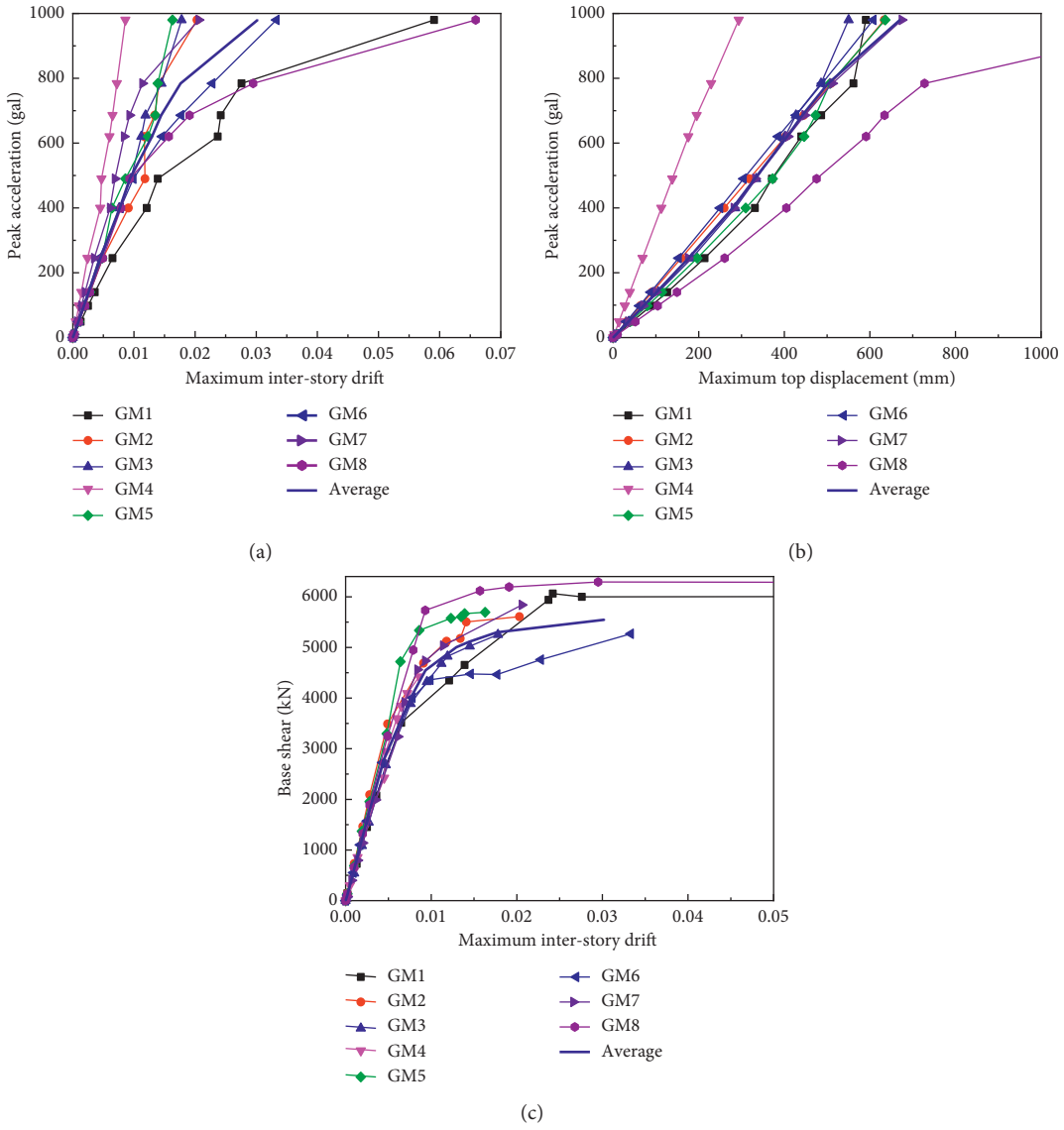

Figure 3: Capacity envelopes of structure: (a) maximum interstory drift; (b) maximum top displacement; (c) base shear-maximum interstory drift curves.

4.1. Capacity Curves of Model M-20-5. In the 8 selected seismic records, peak acceleration increased to 1.0 g, and the capacity curves of model M-20-5 were analyzed using the IDA method in OpenSees. The capacity curves of M-20-5 under different ground motions are shown in Figure 3. The structural response increases gradually with increasing peak acceleration. Even when the acceleration is greater than the corresponding acceleration in the number 9 seismic fortification zone (the design basic acceleration is 0.4 g), the structure maintains good seismic performance.

Peak acceleration reaches 0.8 g under the artificial seismic curve and GM1, and story displacement angle increases rapidly, indicating the structure will collapse. Under other seismic curves, when the peak acceleration reaches approximately 1000gal, the structure maintains good seismic performance; hence, the anticollapse capacity of M-20-5 is 800gal.

4.2. Distribution of Interstory Drift. The envelope of interstory drift of M-20-5 under frequently occurring, moderate, and rare earthquakes is shown in Figure 4. The change of structural maximum interstory drift under frequently occurring earthquakes for varying height of structure is small (maximum interstory drift is less than 4/1000). The average value in this situation is 0.26%, and the average value of maximum interstory drift during a moderate earthquake is 0.77%. The average value of maximum interstory drift during a rare earthquake is 1.3%. The model maximum interstory drift under frequently occurring and rare earthquakes can satisfy deformation requirement for elastic and elastic-plastic in the "Code for seismic design of buildings," which is less than 1/300 and 1/50, respectively. It also satisfies the requirement for moderate earthquake fortification standards ($0.004\,h$–$0.008\,h$) (h is story height) in the "General rule."

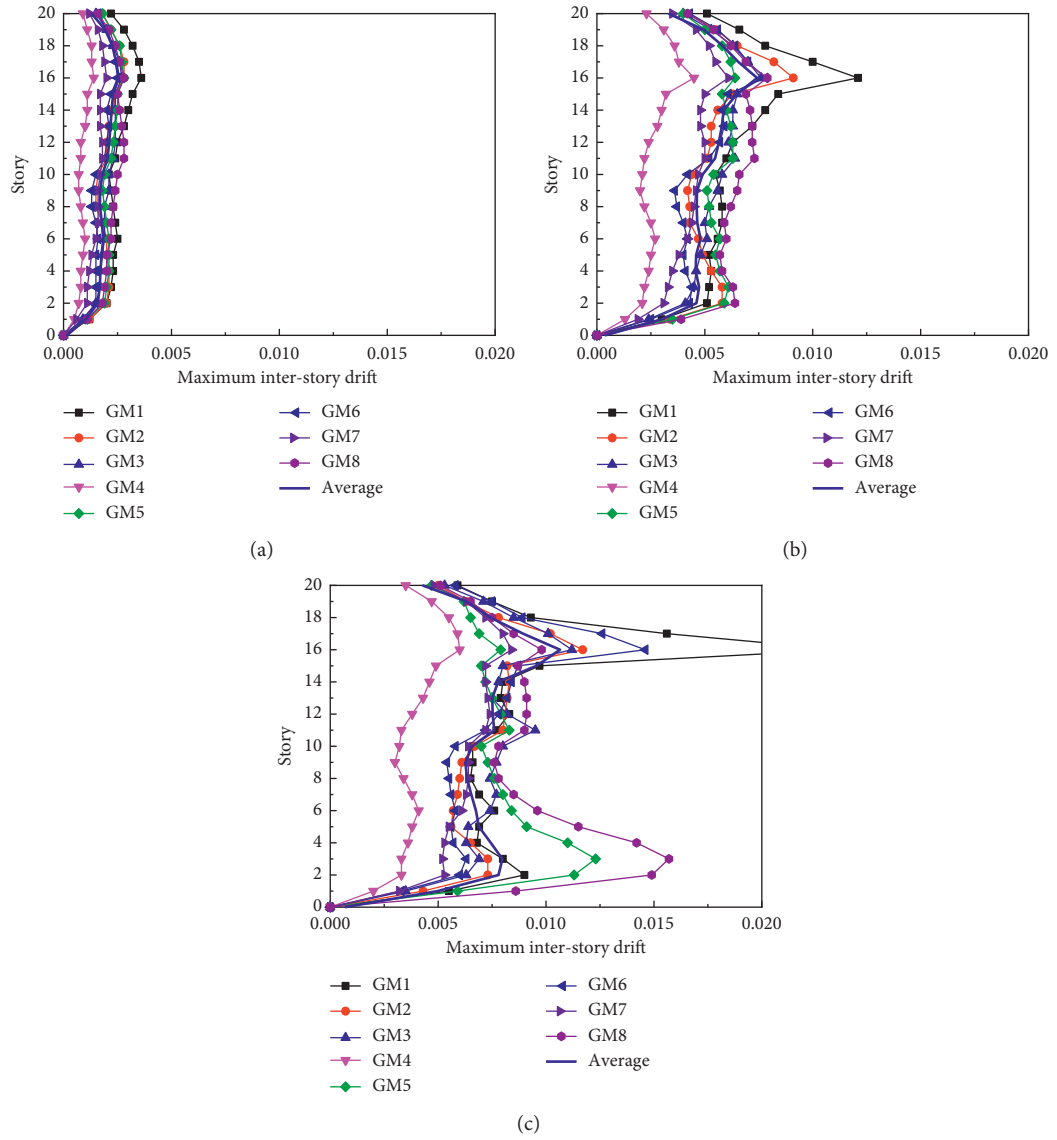

Figure 4: The maximum interstory drift with height of the structure under different seismic waves: (a) frequently occurring earthquake; (b) moderate earthquake; (c) rare earthquake.

Furthermore, the structural maximum interstory drift under frequently occurring and moderate earthquakes changes inconspicuously with height; however, these changes are significant in the bottom and middle-upper sections during rare earthquakes. The maximum interstory drift occurs at the 16th floor primarily because the structural members dimension as well as the stiffness is reduced at this floor. Under frequently occurring earthquakes, the structure is completely elastic, and under moderate earthquakes, the steel plates, acting as energy dissipation elements, yielded first and become plastic hinges to consume energy. In addition, the steel plates also absorb earthquake energy and prevent structural failure. Under rare earthquakes, numerous SPSWs and frame beams yielded to form plastic hinges; however, the structure does not collapse. After yielding, the maximum interstory drift decreased with increasing peak acceleration primarily because the location and order of structural plastic hinge change after the peak acceleration, resulting in internal force redistribution and changing the structure force transfer paths (Figure 4(a)). All of these research results show that CFST frame-SPSWs exhibit good seismic capacity.

4.3. Analysis of Structural Capacity Curve. The 8 capacity curves of maximum interstory drift-base shear for different models under ground motion are shown in Figure 5. The structural seismic response on elastic phase under different ground motions is close to each other (Figure 5). Shear force increases with increasing peak acceleration until the structure yielded into the elastic-plastic phase. Then, the difference in structural response under different ground motions is larger, and the average values from the seismic

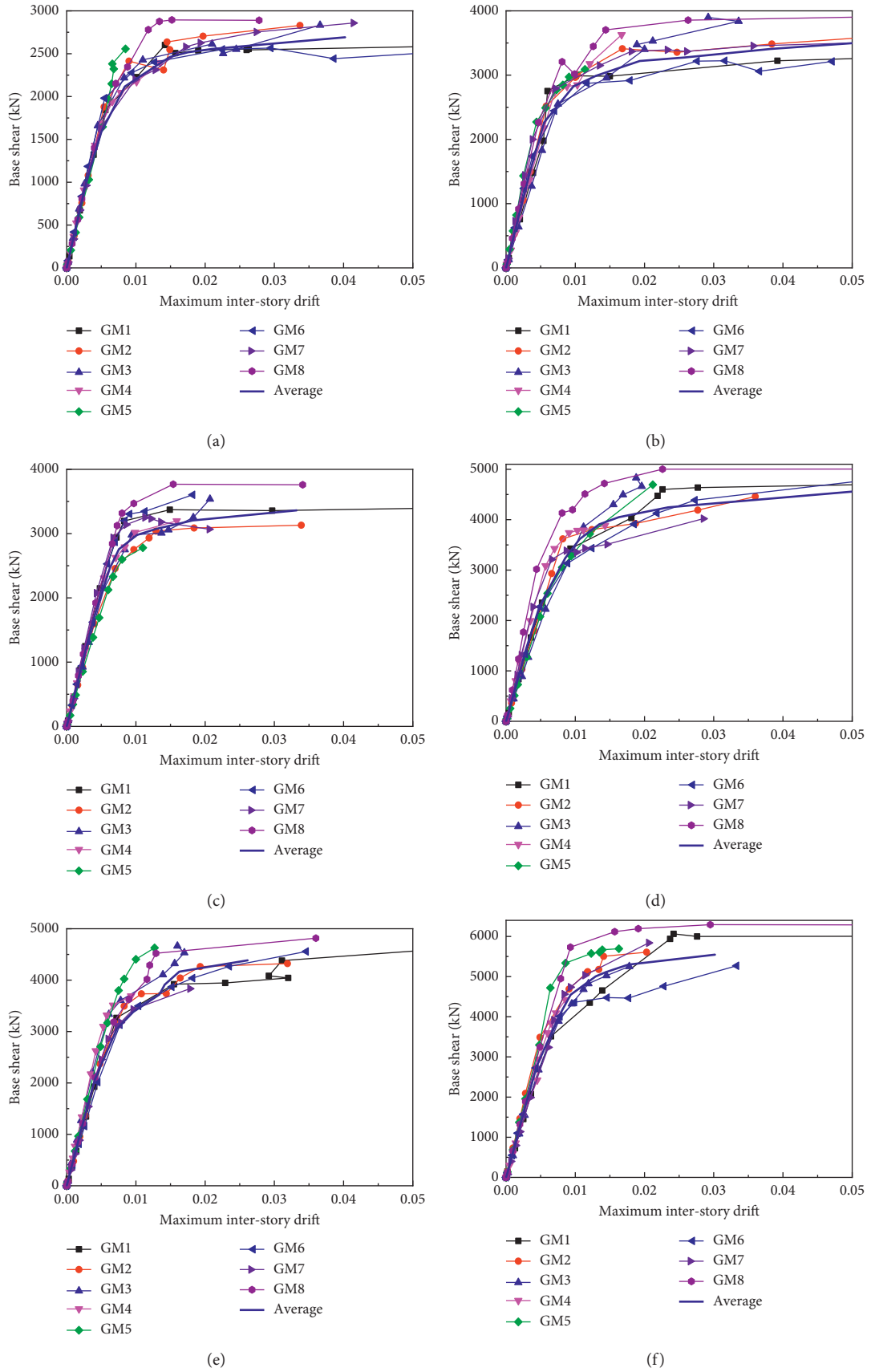

Figure 5: Capacity envelopes of structures for a 9 seismic intensity: (a) Model M-10-3; (b) Model M-10-5; (c) Model M-15-3; (d) Model M-15-5; (e) Model M-20-3; (f) Model M-20-5.

Table 4: Structural performance factors.

Model number	Structural basis period T/s	Structural ductility reduction factor R_μ	Structural overstrength factor R_s	Structural response modification factor R	Displacement amplification factor C_d
M-10-3	1.06	1.254	2.660	3.326	3.194
M-10-5	1.25	1.352	2.402	3.248	3.117
M-15-3	1.57	1.106	2.881	3.187	3.129
M-15-5	1.79	1.192	2.669	3.180	3.056
M-20-3	1.99	1.046	2.938	3.073	2.988
M-20-5	2.19	1.084	2.794	3.029	2.826
Average		1.172	2.724	3.174	3.052
Standard deviation		0.106	0.176	0.098	0.119
Variation coefficient		0.090	0.065	0.031	0.039

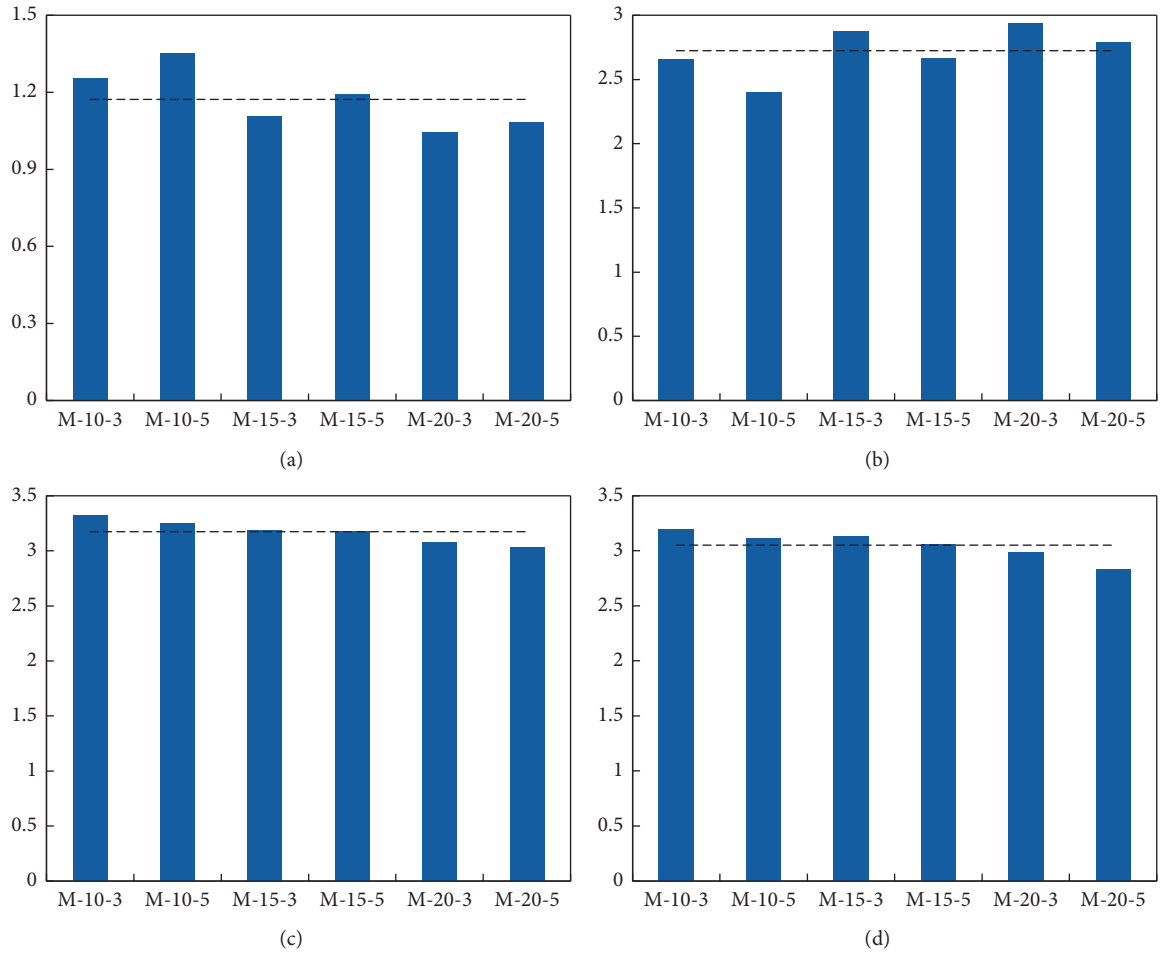

Figure 6: Structural performance factors: (a) structural ductility reduction factor R_μ; (b) structural overstrength factor R_s; (c) structural response modification factor R; (d) displacement amplification factor C_d.

records are adopted to reveal the structural performance. Although the seismic peak acceleration increased to 1.0 g, the structural maximum interstory drift is still less than 2% under the partial ground motions. Results show that CFST frame-SPSWs exhibit good seismic performance, and the structural seismic response is relatively large under the artificial seismic waves. When the peak acceleration increases to 0.8 g, interstory drift increases rapidly, and the structural anticollapse capacity reaches approximately 800 gal.

5. Analysis of Structural Performance Coefficient

For each model, the calculated results R, R_μ, R_s, and C_d are listed in Table 4. The comparison of structural performance

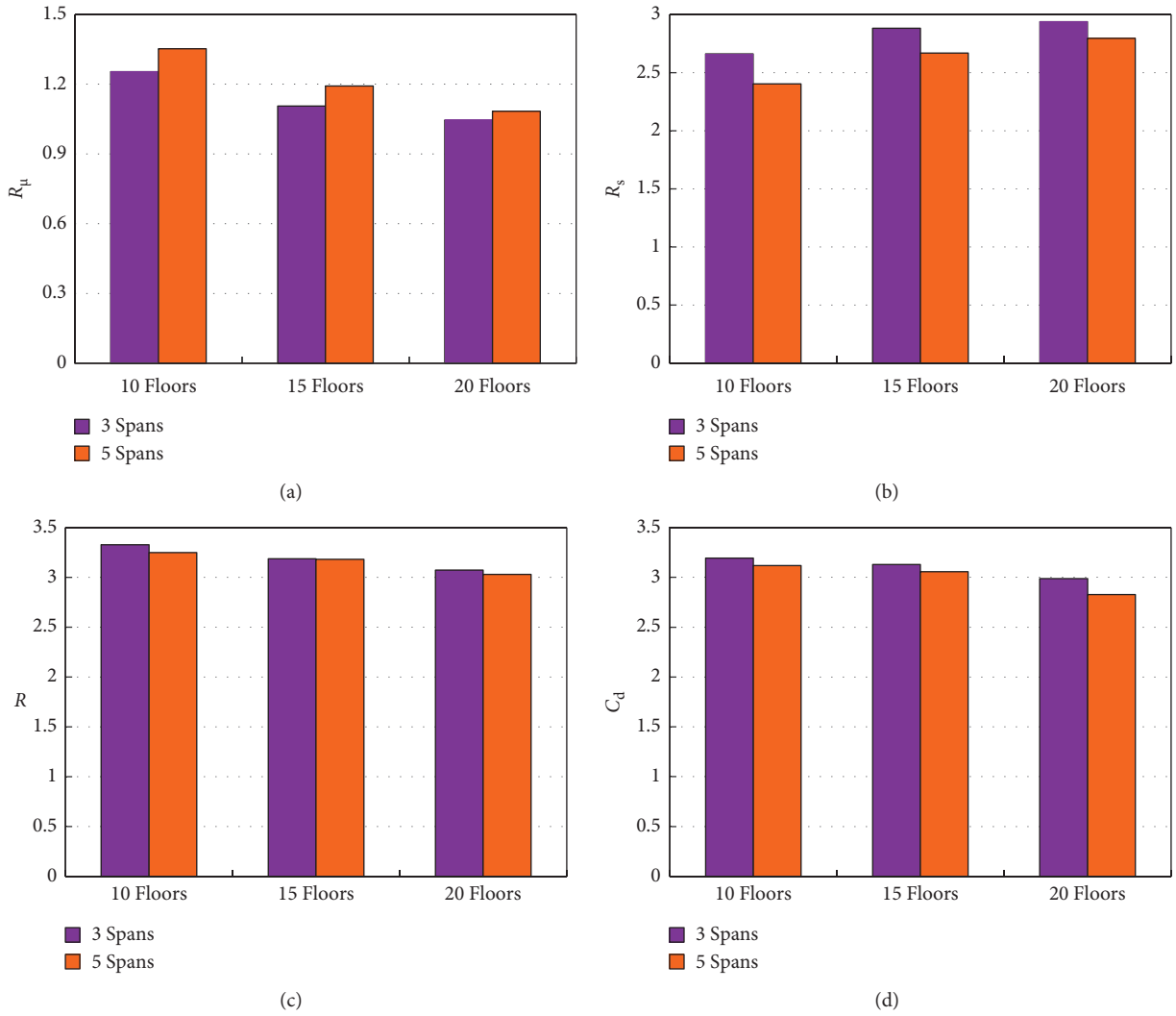

Figure 7: Influence of span number on structural performance factors: (a) structural ductility reduction factor R_μ; (b) structural overstrength factor R_s; (c) structural response modification factor R; (d) displacement amplification factor C_d.

coefficients and their corresponding calculated average values is shown in Figure 6.

The structural performance coefficient changes with changing story number, span number, and structural period (Figure 6). For the models in this contribution, the average values of R, R_μ, R_s, and C_d are 3.194, 1.172, 2.274, and 3.052, respectively. The Chinese "Code for seismic design of buildings" implies that the structural response modification factor is 2.81. The structural response modification factor and displacement amplification factor of CFST frame-SPSW are regulated the same as concrete frame in the "General rule," and their values are 2.63 and 2.2, respectively. The CFST frames-SPSWs have a good seismic performance, and the structural performance coefficient currently used in Chinese code is conservative. This contribution can offer some reasonable suggestions regarding the design and research on some performance coefficients and structural response modification factors. If this result, R is 3.194, is adopted, the designed seismic action will decrease 12% compared with the "Code for seismic design of buildings." Compared with the "General rule," the designed action will decrease 17.7%.

5.1. Influence of Period. The influence of structural period on structural ductility reduction factor R_μ, structural overstrength factor R_s, structural response modification factor R, and displacement amplification factor C_d is shown in Figure 6. As the number of spans and floors of the structure increases, the period of the structure keeps increasing, but for R_μ and R_s, this phenomenon is not significant (Table 4). In addition, R and C_d decrease slightly with increasing structural period.

5.2. Influence of Span Number. The influence of span number on R_μ, R_s, R, and C_d is shown in Figure 7. R_μ increases with increasing span number, but the extent decreases gradually with increasing structural height. R_s decreases with

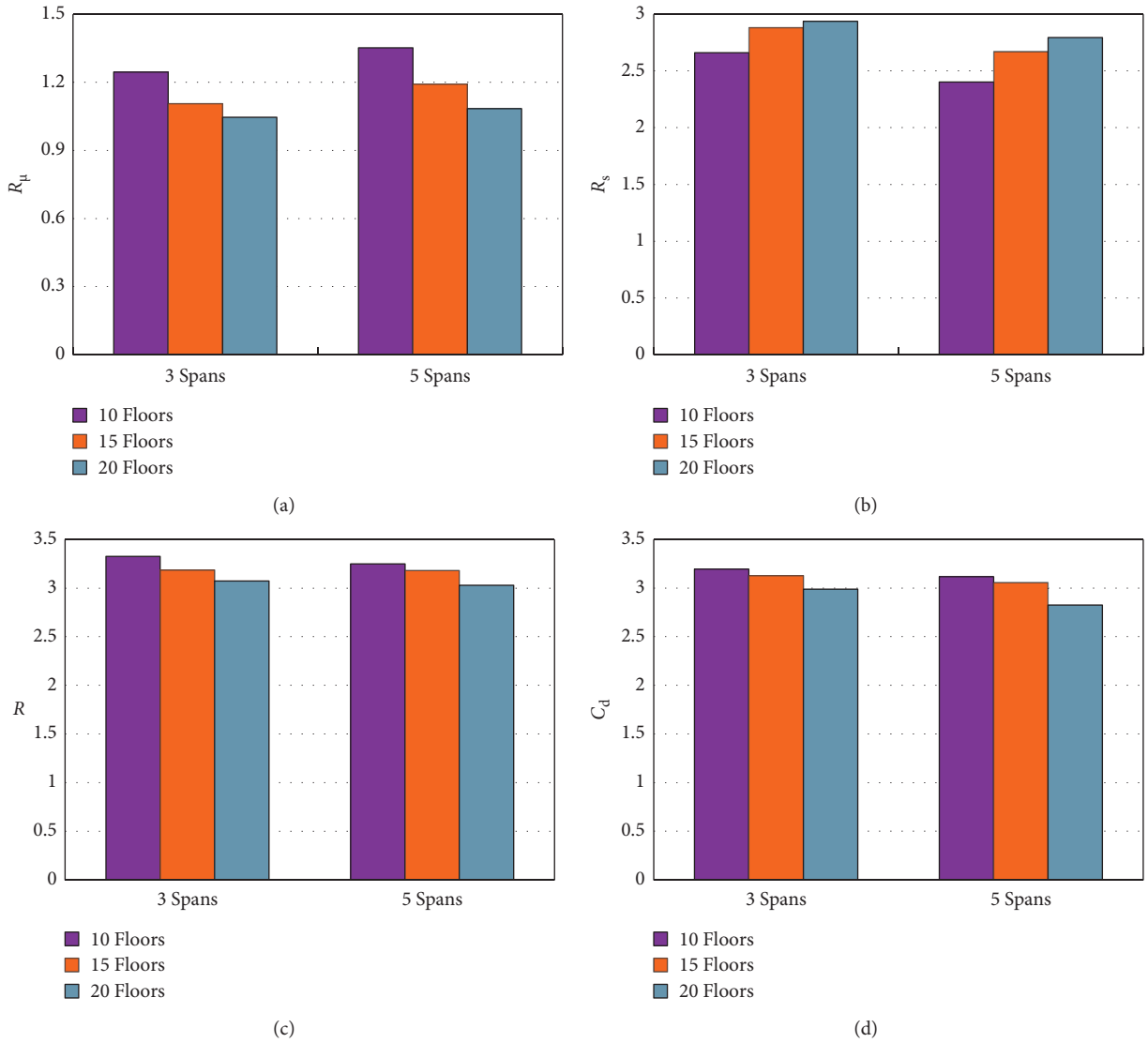

FIGURE 8: Influence of story number on structural performance factors: (a) structural ductility reduction factor R_μ; (b) structural overstrength factor R_s; (c) structural response modification factor R; (d) displacement amplification factor C_d.

increasing span number, but this trend still decreases with increasing structural height. Both R and R_s decrease with increasing span number, and the maximum variable magnitude is 5%, indicating that there is a minor influence between span number and structural performance coefficients within a given period.

5.3. Influence of Story Number. The influence of story number on R_μ, R_s, R, and C_d is shown in Figure 8. R_μ, R, and C_d decrease with increasing story number, and R_s increases with increasing story number. This trend decreases gradually with increasing structural height for all 4 of these coefficients.

6. Conclusions

The nonlinear finite element software OpenSees is adopted to develop the model for CFST frame-SPSWs connected with beams only. These models evaluate structural seismic performance using the IDA method and analyze governing factors, such as R and C_d. The following conclusions can be drawn:

(1) The SPSWs as energy dissipation elements yielded firstly to form plastic hinges under moderate earthquakes. In addition, most SPSWs and frame beams yielded under rare earthquakes, but the structure is not collapse.

(2) R and C_d decrease gradually with increasing story number, span number, and structural period. R_μ increases with increasing span number but decreases with increasing story number. R_s decreases with increasing span number but increases with increasing story number.

(3) The obtained overstrength factor R_s and structural ductility reduction factor R_μ of CFST frame-SPSWs are 2.72 and 1.17, respectively.

(4) The recommended value of response modification factor and displacement amplification factor for CFST frame-SPSWs is 3.17 and 3.05, respectively. The recommended R is greater than the value (2.8) in the "Chinese Code for seismic design of buildings" for composite structures, which indicates the code is conservative.

Nomenclature

C_d: Displacement amplification factor
R: Response modification factor
R_μ: Ductility reduction factor
R_s: Overstrength factor
T: Structural basis period
V_d: Designed base shear
V_e: Maximum base shear when the structure remains completely elastic under moderate earthquake
V_y: Base shear when the structure yields
$\Delta_{\max}$: Maximum top horizontal displacement of the structure during a moderate earthquake
Δ_d: Top horizontal displacement related to the designed base shear
Δ_y: Top horizontal displacement when the structure yields.

Data Availability

The data used to support this study are available upon request to the corresponding author (e-mail: houxiaomeng@gmail.com).

Conflicts of Interest

The authors declare that there are no conflicts of interest.

Authors' Contributions

Qin Rong investigated the study, developed the methodology, provided software, performed formal analysis, wrote original draft, and reviewd and edited the manuscript. Zhonghui Zhao investigated the study and reviewed and edited the manuscript. Lanhui Guo investigated the study and reviewd and edited the manuscript. Xiaomeng Hou developed the methodology, performed formal analysis, reviewed and edited the manuscript, and was responsible for funding acquisition. Li Lin reviewed and edited the manuscript. Hongtao Bi investigated the study and reviewed and edited the manuscript.

Acknowledgments

This contribution was supported by the National Natural Science Foundation of China (No. 52078169), Excellent Youth Foundation of Heilongjiang Province (No. YQ2019E028), Outstanding Young Talents Project of Harbin University of Science and Technology (No. LGYC2018JQ018), and University Nursing Program for Young Scholars with Creative Talents in Heilongjiang Province (No. 8607-324018601).

References

[1] Q. Rong, X. M. Hou, and C. Ge, "Quantifying curing and composition effects on compressive and tensile strength of 160–250 MPa RPC," *Construction and Building Materials*, vol. 241, Article ID 117987, 2020.

[2] Association Standard of Engineering Construction Standardization of China, *CECS 160:2004 General Rule for Performance-Based Seismic Design of Buildings*, China Planning Press, Beijing, China, 2004.

[3] National Standard of the People's Republic of China, *GB50011-2010 Code for Seismic Design of Buildings*, China Architecture and Building Press, Beijing, China, 2010.

[4] C. M. Uang, "Establishing R (or rw) and Cd factors for building seismic provisions," *Journal of Structural Engineering*, vol. 117, no. 1, pp. 19–28, 1991.

[5] A. Whittaker, G. Hart, and C. Rojahn, "Seismic response modification factors," *Journal of Structural Engineering*, vol. 125, no. 4, pp. 438–444, 1999.

[6] A. S. Elnashai and B. M. Broderick, "Seismic response of composite frames-II. Calculation of behaviour factors," *Engineering Structures*, vol. 18, no. 9, pp. 707–723, 1996.

[7] J. Kim and H. Choi, "Response modification factors of chevron-braced frames," *Engineering Structures*, vol. 27, no. 2, pp. 285–300, 2005.

[8] M. Mahmoudi and M. Zaree, "Evaluating response modification factors of concentrically braced steel frames," *Journal of Constructional Steel Research*, vol. 66, no. 10, pp. 1196–1204, 2010.

[9] B. Asgarian and H. R. Shokrgozar, "BRBF response modification factor," *Journal of Constructional Steel Research*, vol. 65, no. 2, pp. 290–298, 2009.

[10] M. Izadinia, M. A. Rahgozar, and O. Mohammadrezaei, "Response modification factor for steel moment-resisting frames by different pushover analysis methods," *Journal of Constructional Steel Research*, vol. 79, pp. 83–90, 2012.

[11] W. A. Attia and M. M. M. Irheem, "Boundary condition effect on response modification factor of X-braced steel frames," *HBRC Journal*, vol. 14, no. 1, pp. 104–121, 2018.

[12] M. Mahmoudi and M. G. Abdi, "Evaluating response modification factors of TADAS frames," *Journal of Constructional Steel Research*, vol. 71, pp. 162–170, 2012.

[13] F. Aliakbari and H. Shariatmadar, "Seismic response modification factor for steel slit panel-frames," *Engineering Structures*, vol. 181, pp. 427–436, 2019.

[14] Q. Gu, Y.-K. Shen, and C. Li, "The seismic response modification factors of steel structures," *Journal of Suzhou University of Science and Technology (Engineering and Technology)*, vol. 24, no. 4, pp. 18–24, 2011.

[15] H. G. Jouneghani and A. Haghollahi, "Assessing the seismic behavior of steel moment frames equipped by elliptical brace through incremental dynamic analysis (IDA)," *Earthquake Engineering and Engineering Vibration*, vol. 19, no. 2, pp. 435–449, 2020.

[16] S. Arthi and K. Jaya, "Seismic performance of precast shear wall-slab connection under cyclic loading: experimental test vs. Numerical analysis," *Earthquake Engineering and Engineering Vibration*, vol. 19, no. 3, pp. 739–757, 2020.

[17] Y. Zhang, P. Pan, R. Gong, T. Wang, and W. Xue, "Substructure hybrid testing of reinforced concrete shear wall structure using a domain overlapping technique," *Earthquake Engineering and Engineering Vibration*, vol. 16, no. 4, pp. 761–772, 2017.

[18] C. H. Zhai, *Research of the Severest Designed Ground Motions and Strengh Reduction Coefficients*, pp. 55–125, Harbin Institute of Technology, Harbin, China, 2004.
[19] S. S. Cui, D. G. Lu, and P. Y. Song, "Effects of infill walls and casting slabs on global overstrengh of RC frames," *Journal of Building Structures*, vol. 35, no. 8, pp. 30–36, 2014.
[20] S. Cui, Y. Chen, and D. Lu, "Probability assessment of structural response modification factor of RC frames by the demand-capacity-factor method," *Structure*, vol. 30, pp. 628–637, 2021.
[21] M. Masoudi, S. Eshghi, and M. Ghafory-Ashtiany, "Evaluation of response modification factor (R) of elevated concrete tanks," *Engineering Structures*, vol. 39, pp. 199–209, 2012.
[22] Aci Committee, *ACI 371R-08. Guide for the Analysis, Design, and Construction of Elevated concrete and Composite Steel-concrete Water Storage Tanks*, American Concrete Institute, Farmington Hills, MI, USA, 2008.
[23] A. Mondal, S. Ghosh, and G. R. Reddy, "Performance-based evaluation of the response reduction factor for ductile RC frames," *Engineering Structures*, vol. 56, no. 6, pp. 1808–1819, 2013.
[24] W. L. Cao, R. W. Wang, F. Yin, and H. Y. Dong, "Seismic performance of a steel frame assembled with a CFST-bordered composite wall structure," *Engineering Structures*, vol. 219, Article ID 110853, 2020.
[25] J. B. Yan, Y. Y. Yan, and T. Wang, "Cyclic tests on novel steel-concrete-steel sandwich shear walls with boundary CFST columns," *Journal of Constructional Steel Research*, vol. 164, Article ID 105760, 2020.
[26] L. Guo, Q. Rong, B. Qu, and J. Liu, "Testing of steel plate shear walls with composite columns and infill plates connected to beams only," *Engineering Structures*, vol. 136, pp. 165–179, 2017.
[27] Q. Rong, Y. H. Zeng, L. H. Guo, X. M. Hou, and W. Z. Zheng, "Response of RPC-filled circular steel tube columns under monotonic and cyclic axial loading," *Shock and Vibration*, vol. 2019, Article ID 9141592, 16 pages, 2019.
[28] Q. Rong, J. Hou, L. H. Guo, and S. M. Zhang, "Structural response modification factor analysis of CFST frame-composite steel plate shear walls with two side connections," *China Civil Engineering Journal*, vol. 49, no. S2, pp. 45–50, 2016.
[29] Q. Rong, *Research of CFST Frame -SPSWs with Two Sides Connections for Seismic Performance*, pp. 133–155, Harbin Institute of Technology, Harbin, China, 2013.
[30] S. Mazzoni, F. McKenna, M. H. Scott et al., *Open System for Earthquake Engineering Simulation User Command- Language Manual*, pp. 145–170, University of California Berkeley, Berkeley, CA, USA, 2004.
[31] M. H. Scott, *Software Frameworks for the Computational Simulation of Structural Systems*, pp. 65–79, University of California, Berkeley, CA, USA, 2004.